

Mass spectrometry imaging reveals uptake of the allergen methylisothiazolinone in ex vivo human skin

Downloaded from: https://research.chalmers.se, 2025-11-28 16:02 UTC

Citation for the original published paper (version of record):

Clancy, A., Munem, M., Lööf, C. et al (2025). Mass spectrometry imaging reveals uptake of the allergen methylisothiazolinone in ex vivo human skin. Microchemical Journal, 219. http://dx.doi.org/10.1016/j.microc.2025.116162

N.B. When citing this work, cite the original published paper.

research.chalmers.se offers the possibility of retrieving research publications produced at Chalmers University of Technology. It covers all kind of research output: articles, dissertations, conference papers, reports etc. since 2004. research.chalmers.se is administrated and maintained by Chalmers Library

ELSEVIER

Contents lists available at ScienceDirect

Microchemical Journal

journal homepage: www.elsevier.com/locate/microc



Mass spectrometry imaging reveals uptake of the allergen methylisothiazolinone in *ex vivo* human skin

Clancy Aoife^a, Munem Marwa^b, Lööf Caroline^b, Hagvall Lina^{c,d}, M. O'Boyle Niamh^a, Malmberg Per^{b,*}

- ^a School of Pharmacy and Pharmaceutical Sciences, Panoz Institute, Trinity College Dublin, D02 PN40, Ireland
- ^b Department of Chemistry and Chemical Engineering Chalmers University of Technology, Gothenburg, Sweden
- Department of Dermatology and Venereology, Institute of Clinical Sciences, Sahlgrenska Academy, University of Gothenburg, Gothenburg, Sweden
- ^d Department of Occupational and Environmental Medicine, Lund University, Lund, Sweden

ARTICLE INFO

Keywords: 2-Methyl-4-isothiazolin-3-one (MI) Contact allergy Skin allergy ToF-SIMS Skin lipids

ABSTRACT

Allergic contact dermatitis (ACD) is a prevalent inflammatory skin condition triggered by allergens such as 2-methyl-4-isothiazolin-3-one (MI), a common preservative. The incidence of contact allergy to MI has fallen in Europe in recent years, attributable to government regulation limiting concentrations of MI I; however, incidence continues to rise in the USA. The pattern and extent of distribution of MI in skin is unknown and a better understanding of the effect of MI on the skin is needed.

In this study NativeSkin Access® human skin biopsies were treated with MI, and Time-of-Flight Secondary Ion Mass Spectrometry (ToF-SIMS) analysis was performed to map the distribution of MI and assess changes in endogenous lipids. MI penetrates the stratum corneum and viable epidermis, with significant lipid alterations observed in the stratum corneum. The use of Argon gas cluster ion beam (Ar-GCIB) sputtering in the ToF-SIMS analysis improved the resolution and clarity of cellular structures, allowing for better visualization of MI penetration and its effects on skin lipids.

The study highlights the utility of ToF-SIMS in combination with Argon gas cluster sputtering in visualizing allergen distribution and its impact on skin lipid composition, providing insights into the mechanisms of skin sensitization.

1. Introduction

Allergic contact dermatitis (ACD) is an inflammatory skin condition caused by an allergic reaction to a substance that comes into contact with the skin, resulting in symptoms like redness, itching, and blisters. [1] It typically occurs within 48–72 h after exposure to the allergen. 2-Methyl-4-isothiazolin-3-one (MI) is a low-molecular weight preservative used in an extensive variety of products including cosmetics, household detergents, paints, metalworking fluids, textiles and plastics, amongst others. [2] Use of MI together with methylchloroisothiazolinone (MCI) in a 1:3 ratio caused a global epidemic of contact allergy in the 1980s. [3] Subsequently, the use of MI alone was introduced in the early 2000s but

MI is also known to be a sensitizer. MI is categorized as a strong sensitizer in the local lymph node assay (LLNA) with an EC3 of 0.4 % in acetone: olive oil.[4] Exposure to MI/MCI in the general population is widespread, as indicated by detection of a mercapturic acid metabolite of MI and MCI in 100 % of sixty persons with no specific exposure to MI or MCI/MI.[5] Structurally, MI contains a five-membered heterocycle with both a nitrogen (N) and sulfur (S) atom in the ring, also containing a conjugated carbonyl moiety (Fig. S1). The N-S bond can react with nucleophiles, e.g., amino acid residues on proteins, which can lead to skin sensitisation. The incidence of contact allergy to MI has fallen in Europe in recent years, attributable to government regulation limiting concentrations of MI and MCI/MI; however, incidence continued to rise

Abbreviations: ACD, Allergic contact dermatitis; API, Active pharmaceutical ingredient; DAG, Diacylglycerol; GCIB, Gas cluster ion beam; MAG, Monoacylglycerol; MALDI, Matrix assisted laser desorption ionization; MI, 2-Methyl-4-isothiazolin-3-one; PBS, Phosphate buffered saline; PCA, Principal component analysis; PC, Phosphatidylcholine; SB, Stratum basale; SC, Stratum corneum; SG, Stratum granulosum; SS, Stratum spinosum; ToF-SIMS, Time of flight secondary ion mass spectrometry; VE, Viable epidermis.

E-mail address: malmper@chalmers.se (P. Malmberg).

^{*} Corresponding author.

in the USA reaching a peak in 2018, but has seen a recent decline. [2,6-9] In the European Union, MI is not allowed in leave-on products, such as skin lotion, and is limited to 0.0015% in rinse-off products, such as shampoo. [10] The pattern and extent of distribution of MI in skin is unknown.

In vitro reconstructed human skin models have been widely used in drug testing, cosmetics and toxicology studies as an alternative to animal testing.[11,12] They usually consist of human keratinocytes and/or fibroblasts. Despite the recent progress that has been made in the reconstruction of more complex skin models containing other cell types, such models still have limitations, as they are not an exact copy of human skin in vivo, and hence the predictability of the human in vivo response remains limited. NativeSkin Access® human ex vivo skin is considered to be highly predictive and cost effective prior to clinical evaluation in humans. NativeSkin Access® consists of human skin biopsies obtained after surgery. Hence, it exhibits normal skin barrier function.[13].

While the effects of MI have been studied extensively using e.g. patch testing (the application of a series of allergens to the patients skin for two days, after which the presence of an eczema-like rash indicates an allergy to the substance)[14], little is known about its distribution in the skin. Studying the distribution of a low-molecular weight compound directly in skin is difficult but recent advances in mass spectrometry imaging (MSI) have demonstrated the possibility to track both allergens, active pharmaceutical ingredients (APIs) and endogenous compounds directly in skin tissue sections.[15-17] While matrix assisted laser desorption ionization (MALDI) based imaging is the dominating technique used for MSI[18,19], time-of-flight secondary ion mass spectrometry (ToF-SIMS) has the potential to chemically map biological tissues and simultaneously localize both endogenous and exogenous compounds at ca 100 nm spatial resolution for conventional ToF-SIMS. [15,20,21] Conventional ToF-SIMS has a limited mass resolution of up to ca 10,000 MRP while Orbi-SIMS can reach resolutions >240,000 at m/z 200 and with spatial resolution down to 2 μ m. [22]. Herein, we use two conventional ToF-SIMS systems, with and without Argon gas cluster sputtering, to study uptake and localization of MI in human ex vivo skin tissue from abdomen and follow endogenous lipid changes caused by MI.

2. Materials and methods

2.1. Methylisothiazolinone

MI (95 %, Merck, CAS: 2682-20-4) was diluted to 0.0175 M (equivalent to the concentration used for diagnostic patch-testing of 0.2 % w/v) in phosphate buffered saline (PBS). For ToF-SIMS analysis of the MI standard a small amount of MI powder was deposited in a clean silicon wafer.

2.2. Ex-vivo skin tissue exposure and preparation

NativeSkin access (11 mm) was cultured in sterile conditions as recommended by the manufacturers. Briefly, samples were incubated in the provided culture medium for at least one hour at 37 °C, 5 % CO₂, and 95 % relative humidity prior to treatment with contact allergens. MI (Merck)(20 μ L, 0.0175 M solution in PBS) was applied to NativeSkin access 11 mm (Genoskin, France)(n=2). PBS (20 μ L) was applied as the vehicle control (n = 2). The experiment was performed on two independent occasions with skin samples from two different donors. Both donors were females, aged 42 years old, with skin type 2 according to Fitzpatrick's classification guidelines[23]. The skin sample from both donors was taken from the abdominal area. The Trinity College Dublin Faculty of Health Sciences Ethics Committee approved the study (ref: 220401).

After skin exposure, the tissue was collected and frozen in liquid nitrogen. The frozen skin tissue was sectioned vertically in a cryostat to a thickness of 10 μ m. Four slices from the middle of the tissue sample were

collected and mounted on conventional glass slides for ToF-SIMS analysis. Four duplicate glasses was prepared for each tissue experiment. At least 4 tissue sections per exposure type were stained using standard Haematoxylin and Eosin staining. The glass slides were kept frozen until analysis, when they were defrosted in the load lock of the TOF-SIMS instrument at a final vacuum of $10e^{-6}$ mbar.

2.3. TOF-SIMS analysis

The ToF-SIMS surface analysis was carried out using two different ToF SIMS 5 instruments (IONTOF GmbH, Münster, Germany). One system was equipped with a 25 keV Bi cluster ion gun as a primary ion source and a 10 keV C60+ source for sputtering (ToF-SIMS system 1). The other system was equipped with a 30 keV bismuth nanoprobe and an Argon gas cluster ion source (Ar-GCIB) (ToF-SIMS system 2). For both systems mass spectra in positive ion mode were acquired by using the bismuth primary ion sources. To acquire images with high spatial respective mass resolution, the delayed extraction mode was used.[24] The pulsed primary ion currents were in the range of 0.11 pA to 0.17 pA using Bi_3^+ ions. Areas of about 100 $\mu m \times 100~\mu m$ to 200 $\mu m \times 200~\mu m$ on the skin section were selected with a raster of 256 \times 256-pixels and analyzed with 100 raster scans. For the ToF-SIMS system 2, sputtering with the Ar-GCIB was performed using Ar1500 at 5000 eV with an ion current of 4.9 nA.

Three different sections from the specimens of control and MI treated samples were analyzed, respectively. The spectra were internally calibrated to signals of common fragments as $[C]^+$, $[CH_2]^-$, $[CH_3]^-$, $[C_5H_{15}PNO_4]^-$, and $[C_{27}H_{45}]^+$.

The MI standards and control skin tissue was analyzed in the spectrometry mode on ToF-SIMS system 2. Here the MI standard was introduced to vacuum and analyzed at multiple time points with a current of 0.4~pA using Bi_3^+ ions.

The software SurfaceLab (version 7.3, IONTOF, Germany) was used to process, record, analyze and evaluate images and mass spectra.

2.4. Statistics

An automated peak selection was used to select m/z values of both the control and MI treated skin in SURFACELAB 7.1 software. The same mass range was selected (m/z 50 to m/z 800) for the stratum corneum and the viable epidermis. Data was imported to SIMCA software (version 1.0, Umetrics, MKS Instruments Ltd.) as ion intensities normalized to the total ion count. Pareto scaling was performed, and analysis was carried out by principal component analysis (PCA).

3. Results and discussion

MI is a small molecule, with the molecular formula C_4H_5NOS (supplementary fig. S1), a molecular weight of 115 and a vapor pressure of 0.062 mmHg at 25 $^{\circ}C[25]$. Prior to analysis of MI in skin samples, and to understand how MI would behave under vacuum conditions, MI was applied on a silicon wafer and run in ToF-SIMS in both positive and negative polarities (negative data is not discussed), to get an indication about its stability and potential fragmentation patterns.

Spectra from the MI standard (supplementary information, fig. S2) showed the molecular ion $[M+H]^+$ from MI at m/z 116.0. The most significant peak in the spectrum was sodium, Na⁺ at m/z 23. Sodium is an easily ionized species in ToF-SIMS, and thus it is usually one of the highest peaks in the positive ion mode. The spectra showed many other potential fragments such as m/z 62.9 and m/z 80.9 that are most likely to come from fragmentation or reaction of MI but these remained unidentified. Even with the vapor pressure of MI, the molecular ion remained fully stable in the vacuum of the ToF-SIMS for up to 5 h. In the skin tissue analyzed a similar stability is to be expected and the samples were analyzed within this timeframe. Hence, we chose to use the m/z 116.0 ion for detection of MI in skin samples as its formation is

independent of the matrix being analyzed.

It should however be noted that the ionization of the molecule could be different inside the skin tissue based on the matrix of the sample. In ToF-SIMS, a primary ion beam bombards the surface of the sample and secondary species are ejected from the sample. Only a small fraction of the ejected secondary species are ionized and detected. [26] The ionization process is strongly affected by the surface and bulk chemistry, *i.e.* the matrix effect. [27,28] In addition, the response of chemicals to the surrounding tissue is very specific and the ion yield of one chemical can be enhanced while the ion yield of another chemical can be decreased. This can make acquired data from biological samples difficult to interpret. [29,30].

3.1. TOF-SIMS analysis of MI in ex vivo human skin without argon sputtering (system 1)

ToF-SIMS was then performed on ex vivo skin tissue samples to study the uptake of MI and the lipid changes that were caused by MI exposure using initially the ToF-SIMS system 1 equipped with the 25 keV bismuth source. This system lacked an Ar-GCIB and the obtained data only reflects the very top monolayers of the surface of the skin tissue crosssection. In ToF-SIMS, a pulsed and focused primary ion beam enables mass spectrometry imaging. When using conventional ToF-SIMS instruments, the focusing modes of the primary ion beam can be adjusted to either get a high mass resolution or high lateral resolution. An alternative method to maintain the mass resolution with high spatial resolution is to extract secondary ions from the sample surface with a certain delay after the arrival of primary ions, i.e. so-called delayed extraction[24]. After identifying the peaks of interest, the delayed extraction imaging method was applied on the skin tissue and the MI molecular ion was located in the MI treated sample as shown in supplementary fig. S3.

The epidermis is the outermost layer of the skin. It consists of four distinctive layers, the superficial stratum corneum (SC), stratum granulosum (SG), stratum spinosum (SS), and the innermost stratum basale (SB). The SG, SS and SB are part of the viable epidermis (VE, thickness: $50-100 \mu m$), whereas the SC (thickness: $10-20 \mu m$) is part of the nonviable epidermis.[31] Fig. S3a reveals the total ion signal which shows a relative homogenous signal across all skin layers. The distribution for MI can be seen in fig. S3d and shows a distribution mainly in the SC but also inside the VE. Very little biologically relevant information could be revealed from the samples except signals from the phosphatidylcholine (PC) head group (m/z 184.1, fig. S3b) and cholesterol (m/z 369.3, fig. S3e). It was not possible to differentiate any clear morphological cell structures. A spectrum from the skin tissue analyzed using ToF-SIMS system 1 equipped with the 25 keV bismuth source using the spectrometry mode can be seen in supplementary information fig. S4. A background signal from m/z 116.0 using spectrometry mode on this system was also seen (supplementary Fig. S7).

3.2. TOF-SIMS analysis of MI in ex vivo human skin with argon GCIB sputtering (system 2)

Additional MI and control samples were run on the ToF-SIMS system 2 instrument using the 30 keV bismuth nanoprobe and Ar-GCIB sputtering. The use of Ar-GCIB sputtering in biological ToF-SIMS imaging has significantly improved the technique by enabling the detection of large biomolecules with minimal sample damage, enhancing sputtering yield, and increasing secondary ion intensity [32–34]. Hence, immediately prior to ToF-SIMS analysis, the samples were sputtered with the Ar-GCIB for 10 s (approx. 4E+14 ions/cm²) to reveal a fresh surface. The sample was then analyzed in the non-interlaced 3D imaging mode using sequential imaging with the bismuth nanoprobe and Ar-GCIB sputtering. The Ar-GCIB sputters the material from the top layer of the sample and allows for improved resolution of the depth profile. The Ar-GCIB is considered superior for biological applications to traditional sputtering

sources like oxygen and cesium due to its ability to distribute ionic energy across a cluster of argon atoms, allowing for softer ionization and reduced damage to the sample.[34] Several peaks of interest were identified from the ToF-SIMS spectra, including PC headgroup fragment ions at m/z 86.1 and m/z 184.1, and a cholesterol fragment ion at m/z 369.3. Multiple monoacylglycerol fragment ions (m/z 311.1, 313.1, 339.1) and diacylglycerol fragments (m/z 577.2, 601.3, 603.2, 605.3) were also observed as shown in supplementary information fig. S5. The MI fragment was identified at m/z 116.0 as discussed earlier.

The localization of the PC, MI, cholesterol and Na_2PO_3 ions is displayed in Fig. 1. The images show clear cellular structures in the VE, including nuclei and phospholipid membranes. This image is comparable to previously published images which visualized GenoSkin biopsies using light sheet fluorescence microscopy. These images show a mature stratum corneum and the dermal-epidermal junction which is comprised of keratinocytes. Similar cellular structures can be seen using this improved ToF-SIMS mass spectrometry imaging technique compared to the initially used Tof-SIMS system 1. Non-homogenous skin structures have also been noted by others using OrbiSIMS and GCIB sputtering. [351.

In Fig. 1c, the Na₂PO₃ at m/z 124.9 can be seen and is also represented in green in the overlay image in Fig. 1f. This was only detected in the upper layers of the VE, most likely the SG and SS and was at its highest intensity in keratinocytes. This indicates that this ion corresponds to a compound that is mainly restricted to the nucleus. Surrounding the cells was the PC headgroup fragment (m/z 184.1, Fig. 1b). This fragment was also only seen in the VE, corresponding with previously published studies that conclude that levels of phospholipids are negligible in the SC.[36] The fragment appeared at its highest intensity on the surroundings of the Na₂PO₃ signal from the cells, indicating that this fragment makes up the phospholipid barrier. The MI ion appeared as a brighter band at the end of the SC layer but also showed a localization similar to the PC headgroup with a low continuous signal across the SC and VE (red in Fig. 1f). The signal from cholesterol could be seen mainly in the SC layer if the skin as shown in Fig. 1 (Cholesterol images from control tissue is seen in supplementary fig. S7).

Analysis of PBS exposed control tissue, also sputtered with Ar-GCIB for 10 s, revealed a low background signal at m/z 116.0 and a larger adjacent peak at m/z 116.1 that could potentially influence the signals in the MI exposed tissue. As this signal was relatively low, and the achieved mass resolution allowed separation of m/z 116.0 and m/z 116.1 the influence was considered to be non-significant as demonstrated in supplementary image S6. The distribution of m/z 116.0 in the control tissue is shown in supplementary fig. S7.

A linescan was generated which shows the intensity of the molecular ion from MI across the skin sample using ToF-SIMS system 1 and 2 as seen in Fig. 2a and b. Linescans were also generated of cholesterol (m/z369) and PC headgroup (m/z 86) to localize the SC and the VE respectively (Fig. S8). The linescan shows the initial accumulation of MI in the SC, and then a substantial increase in intensity at about 30–40 μm into the skin sample, representing the penetration of MI into the VE. The increase corresponds to the more intense MI signal that appears to penetrate the keratinocytes in the upper layers of the VE. The intensity of the ion then levels out and decreases slightly as the scan reaches the depths of 130–140 μm , representing the lower layers of the VE. The results from the line scan from the TOF-SIMS system 2 (Fig. 2b) using Ar-GCIB sputtering gives a clearer view of the penetration and shows an overall higher level of the ion also within the VE that was more difficult to see without Ar-GCIB sputtering. The initially high signal of MI on the SC is however lower after GCIB sputtering, indicating that sputtering affects the SC layer differentially than the VE layer.

This effect on the diminishing cholesterol signal in the SC could also be seen when applying a higher Ar ion dose to the skin tissue. Fig. 3 shows another example of MI exposed tissue where a higher Ar sputter dose of 5.3e14 ions/cm² was applied. The total ion and phosphatidylcholine appear unaffected (Fig. 3a and b), while the signal from

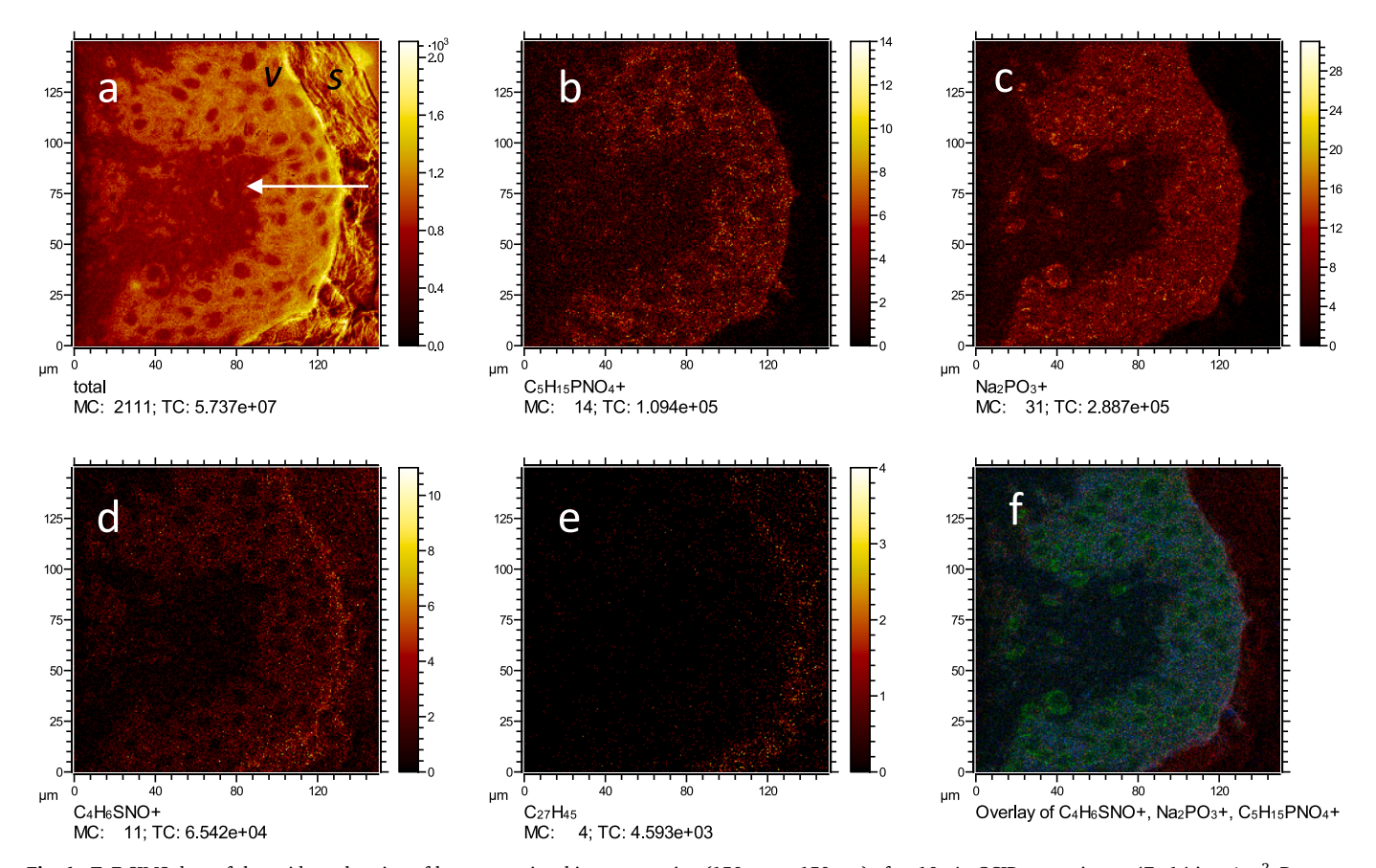


Fig. 1. ToF-SIMS data of the epidermal region of human *ex vivo* skin cross section (150 μ m \times 150 μ m) after 10s Ar GCIB sputtering to 4E+14 ions/cm². Data was acquired using system 2. Ion images of (a) total ion: arrow shows direction of penetration of MI into the skin; (b) phosphatidylcholine (PC) head group (m/z 184.1); (c) Na₂PO₃ nuclear fragment (m/z 124.9); (d) MI molecular ion (m/z 116.0); (e) cholesterol, SC marker (m/z 369.3); (f) a three-colour ion image of the MI fragment (in red), Na₂PO₃ nuclear fragment (in green), and PC (in blue, VE marker). VE: viable epidermis, SC: stratum corneum. (For interpretation of the references to colour in this figure legend, the reader is referred to the web version of this article.)

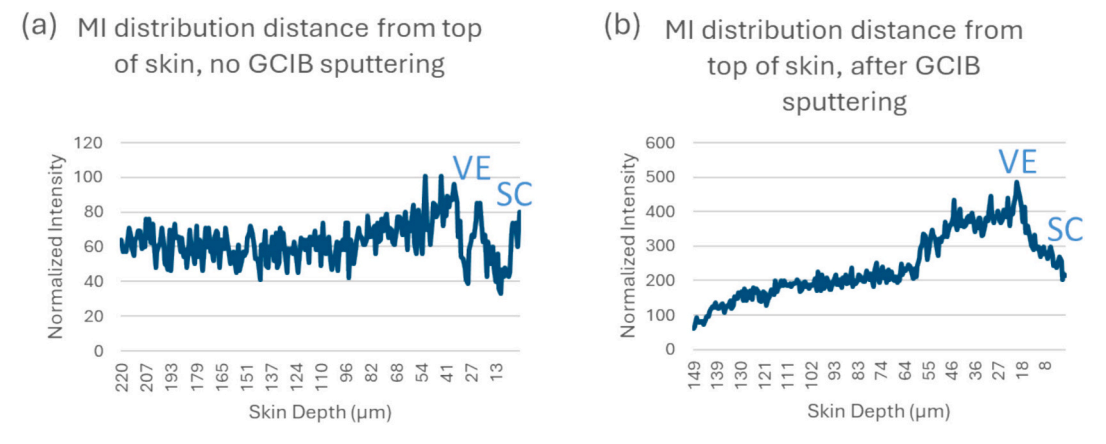


Fig. 2. Linescans of the MI molecular ion (m/z 116.0), showing penetration of MI as a function of penetration depth (distance) from the top/edge of the skin tissue section into the epidermis and dermis by (a) ToF-SIMS system 1 and (b) ToF-SIMS system 2 with Ar-GCIB sputtering.

cholesterol in the SC is fully depleted (Fig. 3e); however, the contrast of the keratinocyte nuclei was much improved (Fig. 3c). The MI signal can still be detected in the SC and the penetration into VE can also be seen adjacent to the keratinocyte nuclei (Fig. 3d and f).

3.3. Effect of MI treatment on endogenous skin lipids

To investigate the effect of MI treatment on endogenous skin lipids, and due to the complexity of lipid composition in different layers of the

skin, the SC and VE layers were analyzed separately. The cholesterol fragment at m/z 369.3 was used as a marker of the SC region, and the PC headgroup fragment at m/z 86.1 was used to identify the VE. Principal component analysis (PCA) suggested that lipid changes were more prominent in the SC rather than the VE of MI-treated samples. In the PCA scores plot (Fig. 4a), t(1) and t(2) denote the sample scores on the first and second principal components, showing how the individual skin samples are distributed according to their overall lipid profiles. The corresponding loadings plot (Fig. 4b) shows p(1) and p(2), which

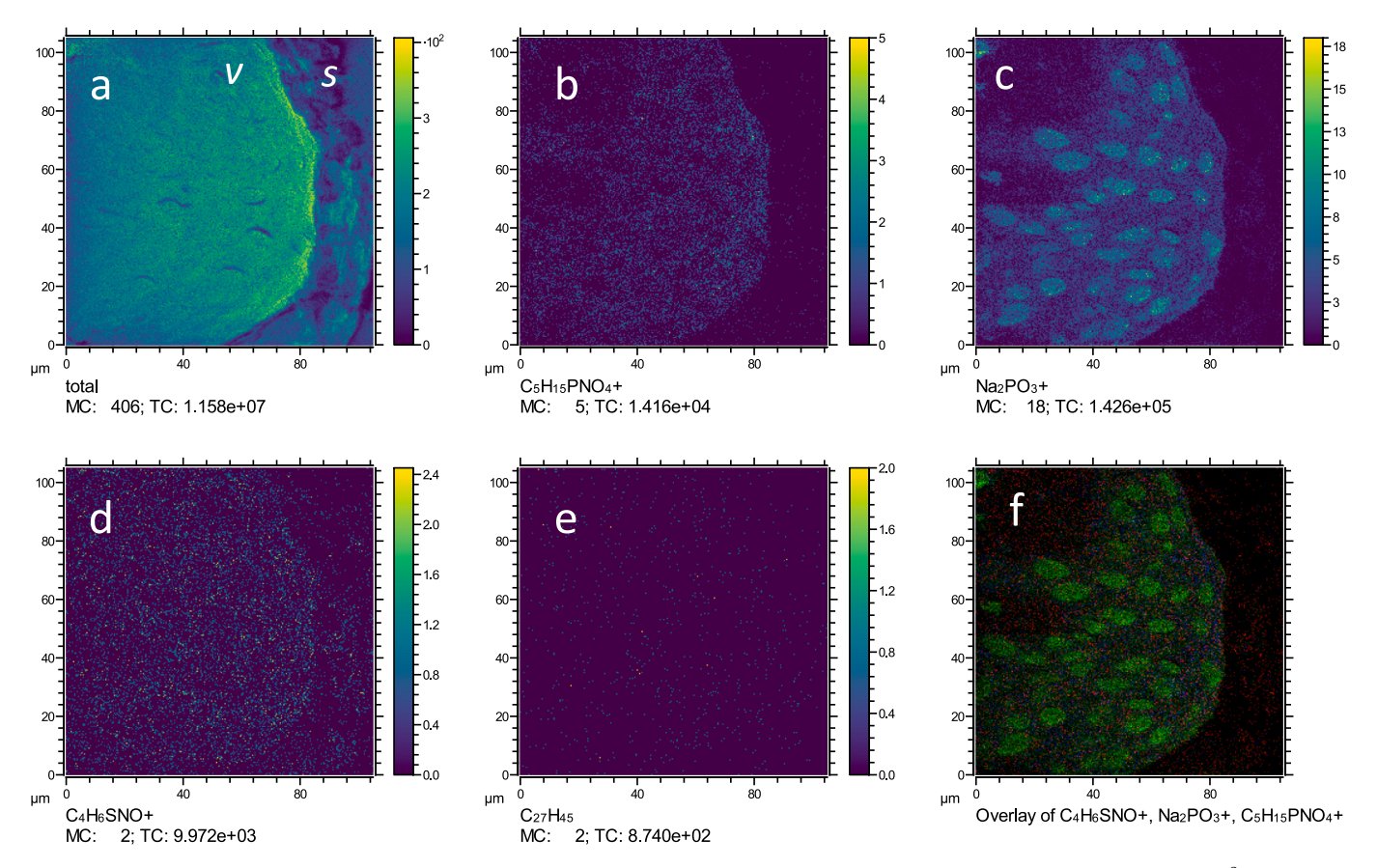


Fig. 3. ToF-SIMS data of the epidermal region of human *ex vivo* skin cross section (105 μ m \times 105 μ m) after Ar GCIB sputtering to 5.3E+15 ions/cm². Ion images of (a) total ion; (b) phosphatidylcholine (PC) head group (m/z 184.1); (c) Na₂PO₃ nuclear fragment (m/z 124.9); (d) MI fragment (m/z 116.0), (e) cholesterol, SC marker (m/z 369.3); (f) a three-colour ion image of the MI fragment (in red), Na₂PO₃ nuclear fragment (in green), and PC (in blue, VE marker). VE: viable epidermis, SC: stratum corneum. (For interpretation of the references to colour in this figure legend, the reader is referred to the web version of this article.)

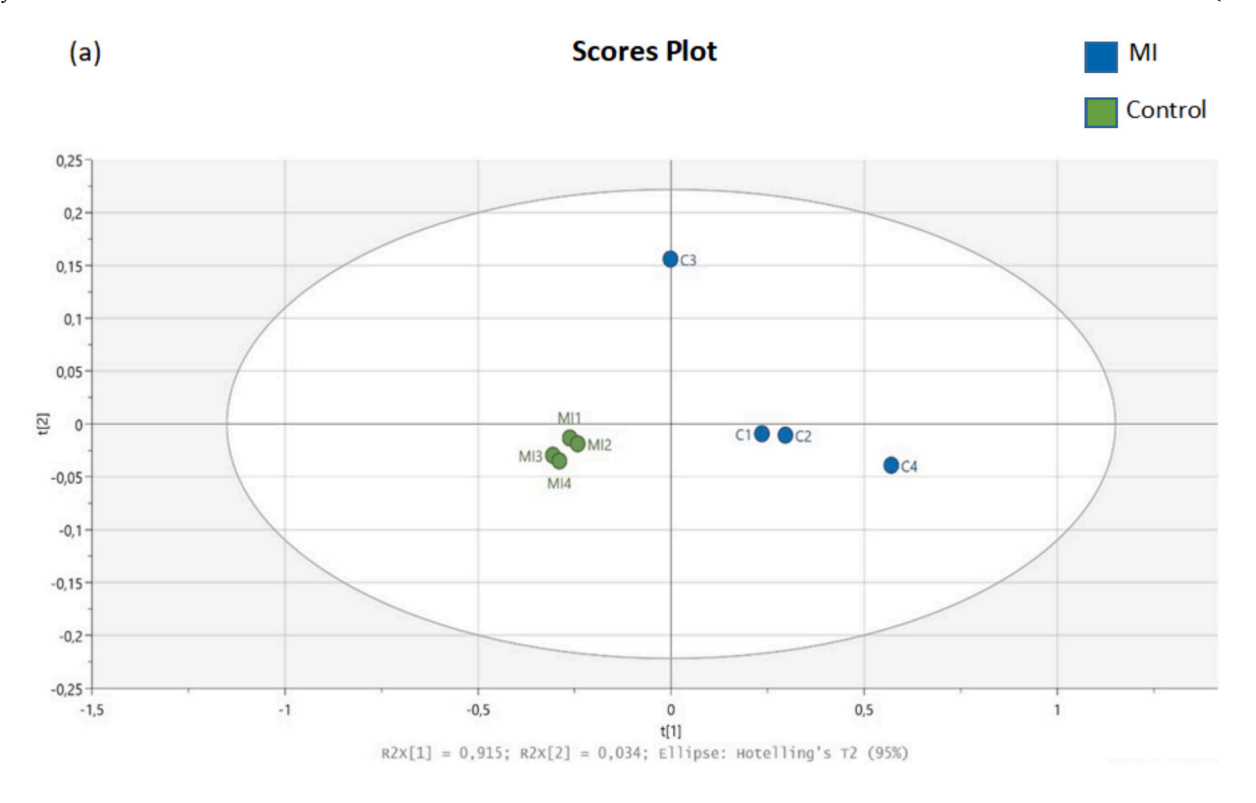
indicate how strongly each m/z feature contributes to these components, thereby highlighting which lipid fragments drive the separation between MI-treated and control samples. In detail, the PCA scores plot identified differences in the chemical composition of the SC of the control (PBS) samples and the treated MI samples [Fig. 4(a)]. The clustering of the MI treated samples (green) in a different quadrant compared to control samples (blue) indicates differences in the chemical makeup of these samples. The loadings plot indicated at which m/z values the most variability between samples was observed. The loadings plot identified changes in PC headgroup fragment at m/z 86.1 (highlighted in blue), as well as some potential differences in diacylglycerol (DAG) content at an m/z of 577.4 (highlighted in red) [Fig. 4(b), magnified version in Fig. S9]. Mass peaks with positive loading values are related to the control samples, while those with negative loading values are related to the MI-treated samples.

To investigate lipid changes in more detail, a selection of ion peaks corresponding to different lipid species were selected and analyzed. Lipid species analyzed included PC headgroup (m/z 86.1 and m/z 184.1, Fig. 5a), cholesterol (m/z 369.3, Fig. 5b), monoacylglycerols (MAGs) (m/z 311.1 and m/z 313.1, Fig. 5c) and DAGs (m/z 577.4 and m/z 601.3, Fig. 5d). The differences in intensities of the peaks at these m/z values in the MI treated samples and controls were analyzed and significant decreases in intensity were seen across many lipid species (Fig. 5).

The intensity of PC headgroup fragments at m/z 184.1 and m/z 86.1 showed a small decrease after treatment with MI, although not statistically significant. It is possible that the decrease correlates with previously published data which showed a decrease in another phospholipid, phosphatidylethanolamine (PE), in bacterial cultures treated with MI [37]. In addition, another sensitizing preservative, sorbic acid, has also

been documented to induce a decrease in PC levels [38]. A decrease in PC headgroup fragment intensity has also been previously documented in the SC after treatment with metal allergens [39]. MI is known to induce an increase in ROS levels[40], which could lead to increased oxidative stress and lipid peroxidation, which could explain the reduction in PC levels observed above. Statistically significant decreases in intensity were however seen across the cholesterol, MAG, and DAG lipid species. DAG ions could also represent triacylglycerols (TAG), as TAG is fragmented in ToF-SIMS to produce mainly DAG ions[41]. As the concentration of MI used in these experiments was equivalent to the concentration used in the patch testing for MI allergy, these lipid changes are of clinical relevance. In the VE, a significant decrease in cholesterol intensity at m/z 369.3 was observed, but there were no significant changes observed across the PC, MAG, and DAG lipid species. Additional ion intensity changes for hydrocarbon fragments are shown in Fig. S10, which shows a variation of increasing and decreasing intensities, indicating that the lipid changes observed upon MI treatment were not due to a matrix effect.

Changes in lipid composition have been previously implicated in the pathophysiology of multiple skin conditions including acne, atopic dermatitis, and psoriasis [42–44]. However, future research is needed to investigate the effect of lipid composition changes in skin sensitization and ACD. Future strategies should include investigation of skin metabolites [45] and lipids in response to MI and also and MALDI MSI at higher mass resolution for more robust lipid analysis to also better understand any matrix effects [46]. Additionally, Future studies should investigate whether the duration of inflammation influences allergen sensitization by altering immune cell engagement rather than simply penetration depth. Specifically, tagging dermal dendritic cells and innate lymphoid



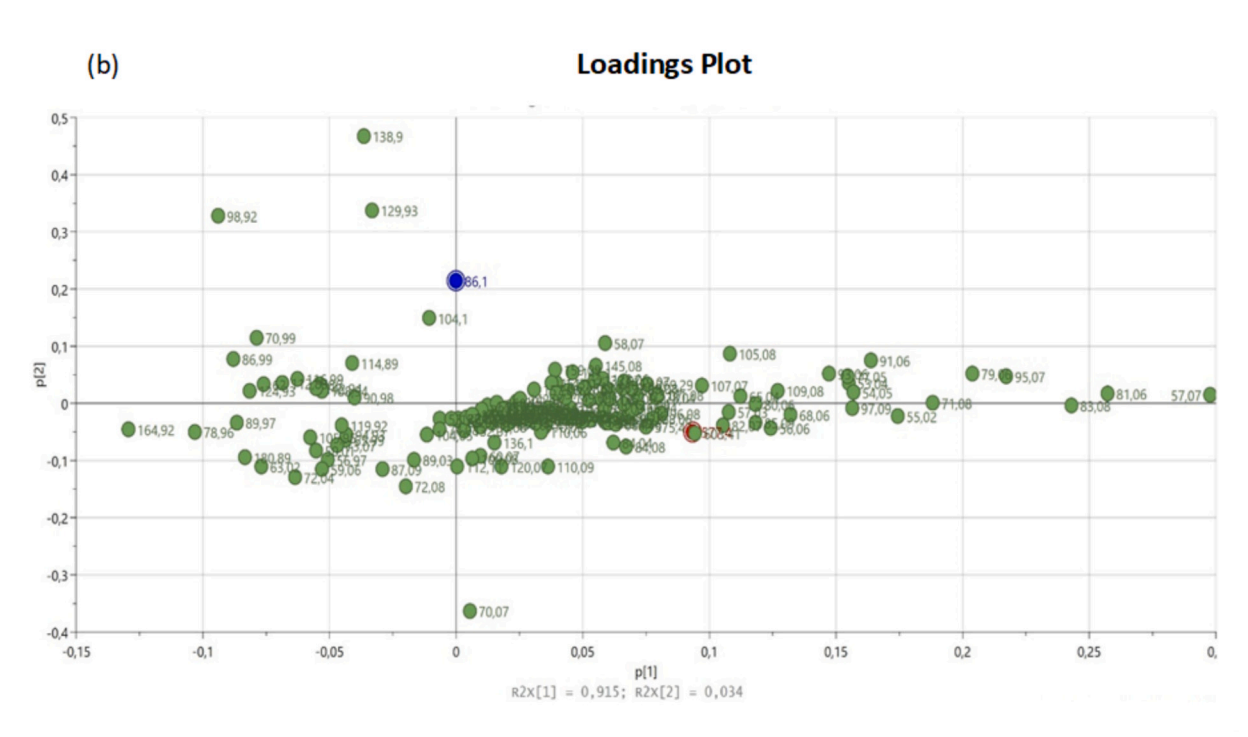


Fig. 4. (a) 2D score plot and (b) loadings plot for PCA of ToF-SIMS data of the SC of MI-treated ex vivo human skin (green) and control (PBS-treated) ex vivo skin (blue). t(1) and t(2) represent the first and second principal components while p(1) and (p2) denote the variable loadings. Data was extracted and analyzed as normalized intensities to total ion count. Scores plot includes all peaks from a range of m/z 50 to 610. Green samples labelled M1/M2/M3/M4 are MI treated samples, and blue samples labelled C1/C2/C3/C4 are control samples. $R^2X[1]$ and $R^2X[2]$ correspond to the proportion of the variance in the data set that is explained by principal component 1 and principal component 2 respectively, in the PCA analysis. (For interpretation of the references to colour in this figure legend, the reader is referred to the web version of this article.)

cells will help determine their proximity to potent allergens such as methylisothiazolinone (MI). Repeating these experiments in chronically inflamed skin with less potent allergens, such as propylene glycol, will clarify whether differences in sensitization are driven by allergen potency or changes in skin immune microenvironment.

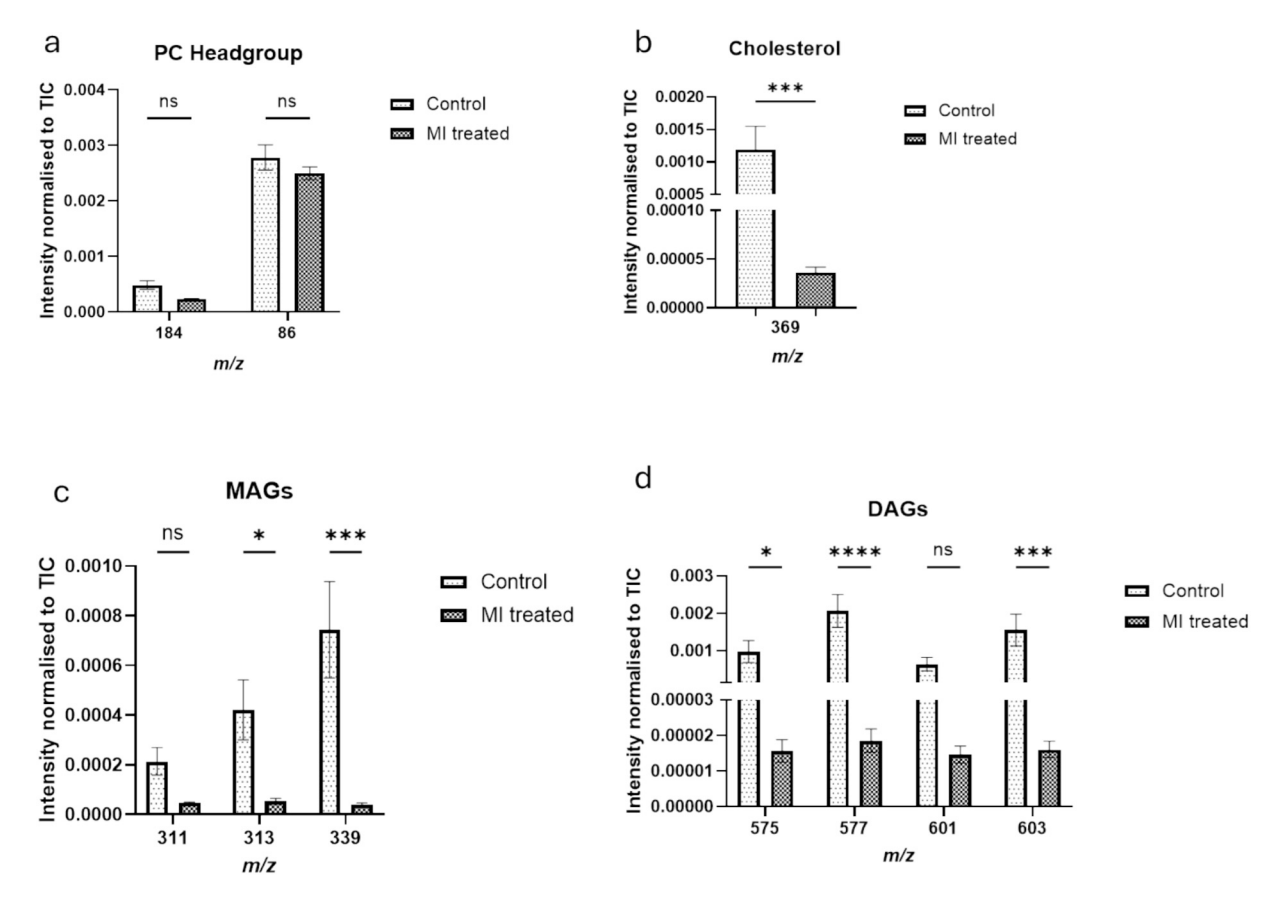


Fig. 5. SC skin lipid analysis for PBS control treated and MI treated *ex vivo* human skin. Data was normalized to total ion count in positive ion mode. Skin was treated with 0.0175 M MI in PBS. Data was analyzed by two-way ANOVA, with Šidák post-hoc test for multiple comparisons. Cholesterol data was analyzed by unpaired students *t*-test. * = p < 0.005, *** = p < 0.001, **** = p < 0.001, *** = p <

4. Conclusions

ToF-SIMS imaging could directly visualize the distribution of 2-methyl-4-isothiazolin-3-one (MI) in human $ex\ vivo\$ skin (Genoskin) using the molecular ion $m/z\$ 116.0. The distribution was clearly seen in the SC layer and extended from the skin surface to about 130–140 μ m inside the skin into the VE region as confirmed by line scans. Sputtering with Ar-GCIB prior to and during analysis resulted in considerably higher clarity of the cellular structures that make up the skin model, and increased clarity of the penetration of MI into the VE and in the regions adjacent to the keratinocytes. Treatment of $ex\ vivo\$ skin with MI resulted in changes in the skin lipid composition of the SC.

CRediT authorship contribution statement

Clancy Aoife: Writing – review & editing, Writing – original draft, Investigation, Formal analysis, Data curation. Munem Marwa: Writing – review & editing, Writing – original draft, Methodology, Investigation, Formal analysis. Lööf Caroline: Writing – review & editing, Writing – original draft, Visualization, Investigation, Data curation. Hagvall Lina: Writing – review & editing, Writing – original draft, Project administration, Funding acquisition, Data curation, Conceptualization. M. O'Boyle Niamh: Writing – review & editing, Writing – original draft, Supervision, Project administration, Funding acquisition, Data curation, Conceptualization. Malmberg Per: Writing – review & editing, Writing – original draft, Supervision, Funding acquisition, Data curation, Conceptualization.

Declaration of competing interest

The authors declare the following financial interests/personal relationships which may be considered as potential competing interests: Per Malmberg reports financial support was provided by Forska utan djurförsök. Niamh O'boyle reports financial support was provided by Analytical Chemistry Trust Fund for a CAMS-UK fellowship. Lina Hagvall reports financial support was provided by The Swedish Skin foundation. If there are other authors, they declare that they have no known competing financial interests or personal relationships that could have appeared to influence the work reported in this paper.

Acknowledgements

The authors would like to thank Nathalie Scheers for kind use of her cell incubator facilities and Ann-Charlott Lindberg for technical assistance. NO'B is grateful to the Analytical Chemistry Trust Fund for a CAMS-UK fellowship (Ref: 600310/07) and to the School of Pharmacy and Pharmaceutical Sciences, TCD for a Panoz Pharmaceutical Innovation PhD Scholarship. LH acknowledges The Swedish Skin foundation (Grant No.: 3037/2020:1 and 2906/2019:1). PM acknowledges Forska utan djurförsök (Grant No.: F2022).

Appendix A. Supplementary data

Supplementary data to this article can be found online at https://doi.org/10.1016/j.microc.2025.116162.

Data availability

Data will be made available on request.

References

- A.-T. Karlberg, M.A. Bergström, A. Börje, K. Luthman, J.L.G. Nilsson, Allergic contact dermatitis—formation, structural requirements, and reactivity of skin sensitizers, Chem. Res. Toxicol. 21 (2008) 53–69, https://doi.org/10.1021/ tv7002239
- [2] A. Herman, O. Aerts, L. de Montjoye, I. Tromme, A. Goossens, M. Baeck, Isothiazolinone derivatives and allergic contact dermatitis: a review and update, J Eur Acad Dermatol Venereol 33 (2019) 267–276, https://doi.org/10.1111/ idv.15267
- [3] M.D. Lundov, M.S. Opstrup, J.D. Johansen, Methylisothiazolinone contact allergy-growing epidemic, Contact dermatitis 69 (2013) 271–275, https://doi.org/ 10.1111/cod.12149.
- [4] European Commission, Directorate general for health and consumers., opinion on methylisothiazolinone (P94) submission II (sensitisation only), Publications Office, LU (2013). https://data.europa.eu/doi/10.2772/7297 (accessed September 29, 2023).
- [5] T. Schettgen, J. Bertram, T. Weber, T. Kraus, M. Kolossa-Gehring, Quantification of a mercapturate metabolite of the biocides methylisothiazolinone and chloromethylisothiazolinone ("M-12") in human urine using online-SPE-LC/MS/ MS, Anal. Methods 13 (2021) 1847–1856, https://doi.org/10.1039/D1AY00183C.
- [6] W. Uter, K. Aalto-Korte, T. Agner, K.E. Andersen, A.J. Bircher, R. Brans, M. Bruze, T.L. Diepgen, C. Foti, A. Giménez Arnau, M. Gonçalo, A. Goossens, J. McFadden, E. Paulsen, C. Svedman, T. Rustemeyer, I.R. White, M. Wilkinson, J.D. Johansen, European environmental contact dermatitis research group, the epidemic of methylisothiazolinone contact allergy in europe: follow-up on changing exposures, J Eur Acad Dermatol Venereol 34 (2020) 333–339, https://doi.org/10.1111/jdv.15875.
- [7] M.J. Reeder, E. Warshaw, S. Aravamuthan, D.V. Belsito, J. Geier, M. Wilkinson, A. R. Atwater, I.R. White, J.I. Silverberg, J.S. Taylor, J.F. Fowler, H.I. Maibach, J. G. DeKoven, T. Buhl, N. Botto, A.M. Giménez-Arnau, R. Gallo, C. Mowad, C.C. V. Lang, V.A. DeLeo, G. Johnston, M.D. Pratt, K. Brockow, B.L. Adler, M.-C. Houle, H. Dickel, M.L.A. Schuttelaar, J. Yu, R. Spiewak, C. Dunnick, F.L. Filon, S. Valiukeviciene, W. Uter, Trends in the prevalence of methylchloroisothiazolinone/methylisothiazolinone contact allergy in north america and Europe, JAMA Dermatol 159 (2023) 267–274, https://doi.org/10.1001/jamadermatol.2022.5991.
- [8] J.F. Schwensen, W. Uter, M. Bruze, C. Svedman, A. Goossens, M. Wilkinson, A. Giménez Arnau, M. Gonçalo, K.E. Andersen, E. Paulsen, T. Agner, C. Foti, K. Aalto-Korte, J. McFadden, I. White, J.D. Johansen, on behalf of the E.E.C.D.R. Group, The epidemic of methylisothiazolinone: a European prospective study, Contact Dermatitis 76 (2017) 272–279, https://doi.org/10.1111/cod.12733.
- [9] M.-C. Houle, J.G. DeKoven, A.R. Atwater, M.J. Reeder, E.M. Warshaw, M.D. Pratt, D.V. Belsito, B.L. Adler, J. Silverberg, J. Yu, N. Botto, C.M. Mowad, C.A. Dunnick, J. S. Taylor, North american contact dermatitis group patch test results: 2021–2022, Dermatitis® (2025), https://doi.org/10.1089/derm.2024.0474.

- [10] CosIng Cosmetics GROWTH European Commission. https://ec.europa. eu/growth/tools-databases/cosing/details/31073, 2023 accessed September 26, 2023
- [11] C. Rasmussen, K. Gratz, F. Liebel, M. Southall, M. Garay, S. Bhattacharyya, N. Simon, M.V. Zanden, K.V. Winkle, J. Pirnstill, S. Pirnstill, A. Comer, B.L. Allen-Hoffmann, The StrataTest® human skin model, a consistent *in vitro* alternative for toxicological testing, Toxicol. *Vitro* 24 (2010) 2021–2029, https://doi.org/10.1016/j.tiv.2010.07.027.
- [12] S. Küchler, K. Strüver, W. Friess, Reconstructed skin models as emerging tools for drug absorption studies, Expert Opinion Drug Metabolism & Toxicol. 9 (2013) 1255–1263, https://doi.org/10.1517/17425255.2013.816284.
- [13] B. Wever, S. Kurdykowski, P. Descargues, Human skin models for research applications in pharmacology and toxicology: introducing nativeskin ®, the "missing link" bridging cell culture and/or reconstructed skin models and human clinical testing, Appl. In Vitro Toxicol. 1 (2015) 26, https://doi.org/10.1089/aivt.2014.0010.
- [14] J.-M. Lachapelle, H.I. Maibach, Patch Testing Methodology, in: J.-M. Lachapelle, H.I. Maibach, J. Ring, U. Darsow, T. Rustemeyer (Eds.), Patch Testing and Prick Testing: A Practical Guide Official Publication of the ICDRG, Springer, Berlin Heidelberg, Berlin, Heidelberg, 2009, pp. 33–70, https://doi.org/10.1007/978-3-540-92,806-5_3.
- [15] P. Sjövall, S. Gregoire, W. Wargniez, L. Skedung, G.S. Luengo, 3D molecular imaging of stratum corneum by mass spectrometry suggests distinct distribution of cholesteryl esters compared to other skin lipids, Int. J. Mol. Sci. 23 (2022) 13799.
- [16] A.M. Handler, M. Fallah, A. Just Pedersen, G. Pommergaard Pedersen, K. Troensegaard Nielsen, C. Janfelt, MALDI mass spectrometry imaging as a complementary analytical method for improved skin distribution analysis of drug molecule and excipients, International Journal of Pharmaceutics 590 (2020) 119949, https://doi.org/10.1016/j.ijpharm.2020.119949.
- [17] J. D'Alvise, R. Mortensen, S.H. Hansen, C. Janfelt, Detection of follicular transport of lidocaine and metabolism in adipose tissue in pig ear skin by DESI mass spectrometry imaging, Anal Bioanal Chem 406 (2014) 3735–3742, https://doi. org/10.1007/s00216-014-7802-z.
- [18] P.J. Hart, S. Francese, E. Claude, M.N. Woodroofe, M.R. Clench, MALDI-MS imaging of lipids in ex vivo human skin, Anal Bioanal Chem 401 (2011) 115–125, https://doi.org/10.1007/s00216-011-5090-4.
- [19] L.H. Cazares, D.A. Troyer, B. Wang, R.R. Drake, O. John Semmes, MALDI tissue imaging: from biomarker discovery to clinical applications, Anal Bioanal Chem 401 (2011) 17–27, https://doi.org/10.1007/s00216-011-5003-6.
- [20] S. Van Nuffel, A. Brunelle, TOF-SIMS Imaging of Biological Tissue Sections and Structural Determination Using Tandem MS, Methods Mol Biol 2437 (2022) 77–86, https://doi.org/10.1007/978-1-0716-2030-4 5.
- [21] S. Aoyagi, T. Matsuzaki, N. Kato, M. Kudo, Chemical imaging of biomolecules in skin using TOF-SIMS and multivariate analysis, JSA 17 (2011) 346–349, https://doi.org/10.1384/jsa.17.346.
- [22] C. Kern, A. Scherer, L. Gambs, M. Yuneva, H. Walczak, G. Liccardi, J. Saggau, P. Kreuzaler, M. Rohnke, Orbi-SIMS mediated metabolomics analysis of pathogenic tissue up to cellular resolution, Chemistry–Methods 4 (2024) e202400008, https://doi.org/10.1002/cmtd.202400008.